

# Specific Binding of Liposomal Nanoparticles through Inverse Electron-Demand Diels–Alder Click Chemistry

Christian Brand,<sup>[a]</sup> Pasquale Iacono,<sup>[a]</sup> Carlos Pérez-Medina,<sup>[b]</sup> Willem J. M. Mulder,<sup>[b, c]</sup> Moritz F. Kircher,<sup>[a, d, e, f]</sup> and Thomas Reiner<sup>\*[a, d, e]</sup>

Here, we report a method to specifically bind liposomal radiopharmaceuticals to a CoCrMo alloy, which can be used in arterial stents, via an irreversible inverse electron-demand Diels–Alder reaction. Inspired by recent accomplishments in pre-targeted imaging using tetrazine-*trans*-cyclooctene click chemistry, we synthesized <sup>89</sup>Zr-labeled *trans*-cyclooctene-functionalized liposomal nanoparticles, which were validated on a tetrazine-appended polydopamine-coated CoCrMo surface. In efforts to ultimately translate this new material to biomedical applications, we compared the ability of <sup>89</sup>Zr-TCO-liposomal nanoparticles (<sup>89</sup>Zr-TCO-LNP) to be immobilized on the tetrazine surface to the control suspensions of non-TCO functionalized <sup>89</sup>Zr-liposomal nanoparticles. Ultimately, this platform technology could result in a systemic decrease of the radiotherapeutic dose deposited in non-targeted tissues by specific removal of long-circulating liposomal radiopharmaceuticals from the blood pool.

Liposomal radiopharmaceuticals have drawn much attention as clinical diagnostics and/or therapeutics in recent years.<sup>[1–5]</sup>

[a] Dr. C. Brand, Dr. P. Iacono, Prof. Dr. M. F. Kircher, Prof. Dr. T. Reiner  
Department of Radiology, Memorial Sloan Kettering Cancer Center  
1275 York Avenue, New York, NY 10065 (USA)  
E-mail: reinert@mskcc.org

[b] Dr. C. Pérez-Medina, Prof. W. J. M. Mulder  
Translational and Molecular Imaging Institute  
Icahn School of Medicine at Mount Sinai  
1470 Madison Ave, New York, NY 10029 (USA)

[c] Prof. W. J. M. Mulder  
Department of Medical Biochemistry, Academic Medical Center  
Meibergdreef 9, 1105 AZ Amsterdam (The Netherlands)

[d] Prof. Dr. M. F. Kircher, Prof. Dr. T. Reiner  
Department of Radiology, Weill Cornell Medical College  
1300 York Avenue, New York, NY 10065 (USA)

[e] Prof. Dr. M. F. Kircher, Prof. Dr. T. Reiner  
Center for Molecular Imaging & Nanotechnology (CMINT)  
Memorial Sloan Kettering Cancer Center  
1275 York Avenue, New York, NY 10065 (USA)

[f] Prof. Dr. M. F. Kircher  
Molecular Pharmacology Program  
Memorial Sloan Kettering Cancer Center  
1275 York Avenue, New York, NY 10065 (USA)

Supporting Information for this article can be found under:  
<https://doi.org/10.1002/open.201700105>.

© 2017 The Authors. Published by Wiley-VCH Verlag GmbH & Co. KGaA. This is an open access article under the terms of the Creative Commons Attribution-NonCommercial-NoDerivs License, which permits use and distribution in any medium, provided the original work is properly cited, the use is non-commercial and no modifications or adaptations are made.

They have been employed as low excretion blood-pool imaging agents, labeled with <sup>18</sup>F,<sup>[2]</sup> as nanoreporters to predict therapeutic outcome during Doxil<sup>®</sup> treatment,<sup>[3]</sup> and as bone marrow imaging agents, tagged with <sup>64</sup>Cu.<sup>[5]</sup> Nanoparticles that are not decorated with a molecularly targeted small molecule, peptide, or antibody can still passively accumulate in tumors, exploiting the enhanced permeability and retention (EPR) effect.<sup>[6]</sup> This increased accumulation of the liposomal radiopharmaceutical in tumor regions allows delineation of tumor margins with positron emission tomography (PET), generally at late time points between 24 and 48 h. However, long-circulating liposomal radiopharmaceuticals tagged with long-lived radionuclides such as <sup>89</sup>Zr and <sup>64</sup>Cu can deposit a significant dose of radiation to non-targeted organs, such as the liver and spleen of patients.<sup>[7]</sup>

Thus, it would be beneficial to utilize early time-point imaging (ideally between 4–6 h post-injection) of long-circulating liposomal nanoparticles so that sufficient tumor signal-to-background ratios can be realized without unnecessary circulation of potentially deleterious radioisotope nanocarriers. We, therefore, designed a liposome-based tetrazine (Tz)/*trans*-cyclooctene (TCO) targeting system by using the inverse electron-demand Diels–Alder (IEDDA) click reaction (Figure 1). Over the last six years, the potential of this reaction has been exploited as a tool for the *in vitro* and *in vivo* labeling of biologically relevant probes.<sup>[8]</sup> This extremely fast ( $k > 30\,000\text{ M}^{-1}\text{ s}^{-1}$ ), selective, and bioorthogonal click reaction<sup>[9]</sup> has been successfully introduced as a pretargeting system for *in vivo* PET imaging<sup>[10]</sup> as well as a radioimmunotherapeutic.<sup>[11]</sup>

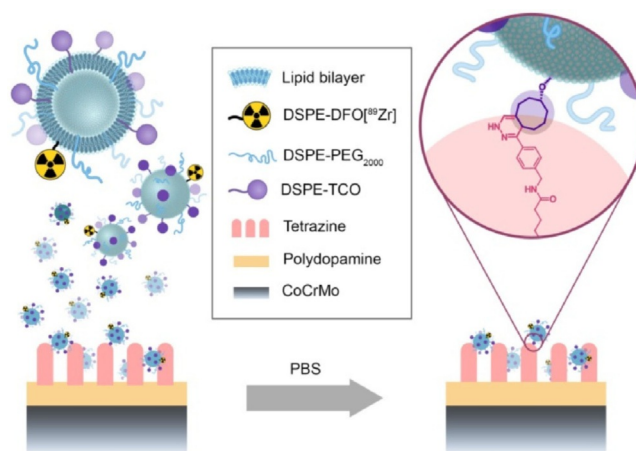


Figure 1. Schematic overview of <sup>89</sup>Zr-TCO-liposome uptake via bioorthogonal inverse electron-demand Diels–Alder click reaction.

In this Communication, we present our recent results towards the development of a platform technology for in vivo removal of a liposomal radiopharmaceutical through the IEDDA reaction. Bioorthogonally reactive liposomes can potentially result in a systemic decrease of the radiotherapeutic dose deposited in healthy tissues, yield a larger therapeutic window, better treatment outcomes, and ultimately more satisfactory prognoses.

To this end, we synthesized  $^{89}\text{Zr}$ -radiolabeled TCO-functionalized liposomes (Figure 2). The preparation of TCO-functionalized liposomal nanoparticles required the synthesis of a derivative of the phospholipid 1,2-distearoyl-*sn*-glycero-3-phosphoethanolamine (DSPE-NH<sub>2</sub>, Figure S1). DSPE-NH<sub>2</sub> was treated with a TCO-functionalized *N*-hydroxysuccinimide (TCO-NHS) ester in the presence of triethylamine to obtain the desired TCO-functionalized phospholipid in moderate yields. After purification, DSPE-TCO was characterized by using mass spectrometry with electrospray ionization (ESI-MS) (Figure S1B). The TCO-functionalized liposomal nanoparticles can then be assembled by using a previously established protocol.<sup>[4]</sup> Together with 1,2-dipalmitoyl-*sn*-glycero-3-phosphocholine (DPPC), cholesterol, DSPE-PEG2000, DSPE-TCO, and DSPE-desferrioxamine (DSPE-DFO), a

high-pressure tip-sonication method yielded the TCO-functionalized liposomal nanoparticle (TCO-LNP) suspension of narrow size distributions (mean diameter =  $109.4 \pm 8.8$  nm, PDI =  $0.153 \pm 0.027$ ). The overall charge of TCO-LNP was measured to be slightly negative, with a zeta potential of  $-6.8 \pm 4.4$  mV. Subsequent radiolabeling of the TCO-LNP surface chelate moieties was achieved through treatment with radioactive  $^{89}\text{Zr}(\text{IV})$ -oxalate (Figure 2A). The desired  $^{89}\text{Zr}$ -radiolabeled TCO-functionalized liposome ( $^{89}\text{Zr}$ -TCO-LNP) was isolated by centrifugal filtration in good radiochemical yield ( $49 \pm 5\%$ ). Size exclusion chromatography (SEC) exhibited high radiochemical purity ( $>97\%$ ) of the radiolabeled, or "hot", liposome population (Figure 2B) with no statistically significant difference in particle size and distributions compared to its "cold" precursor (Figure 2C). Biodistribution studies in 4T1-tumor-bearing nude mice showed typical pharmacokinetics of PEGylated liposomal nanoparticles with increasing ratios of tumor to blood over 24 h of up to  $3.12 \pm 0.57$  (Figure 2D and Figure S2). It is important to note that while tumor/blood ratios increase between 6 and 24 h, sufficient tumoral uptake of  $^{89}\text{Zr}$ -TCO-LNPs was observed as early as the 6 h time point. In fact, the mean percent injected dose per gram ( $\% \text{ID g}^{-1}$ ) of tumoral tissue actually decreases between 6 and 24 h ( $17.0 \pm 4.2$  and  $14.0 \pm 1.2 \% \text{ID g}^{-1}$  for 6 and 24 h, respectively). Enhanced contrast should not only be achieved by increased particle accumulation, but rather clearance of  $^{89}\text{Zr}$ -TCO-LNPs from the blood pool. A rapid route for selective tracer removal from the blood pool would, therefore, decrease the radiation dose as well as allow for earlier imaging time points.

Rationally, a tetrazine-functionalized polydopamine-coated CoCrMo stent alloy was prepared so that bioorthogonally selective removal of  $^{89}\text{Zr}$ -TCO-LNPs can be realized (Figure 3). The inherent chemical robustness of these particular alloys allows them to be suitable as core materials for frameworking arterial stents. The noble metal surface character of these alloys also suggests that a thorough oxidation treatment can allow for a subsequent treatment with a functionalized organic substrate through the resulting strong Van der Waals forces and covalent interactions between the substrate and the metal. Recent preparations of polydopamine (PDA)-coated CoCr alloys utilized such strategies to install functional amines on the metal surface primarily through the chelating catechol moieties of the dopamine monomer.<sup>[12]</sup> These functional handles were ultimately employed as linkers to slow-releasing crosslinked cyclodextrins for drug delivery, although PDA and its polymeric analogues can be utilized in many other applications.<sup>[13]</sup> In this report, a PDA-coated CoCrMo alloy was prepared by peroxide-mediated surface oxidation, rendering the metal surface reactive to the catechol groups on dopamine molecules (Figure 3A). Subsequent thermal treatment cured the surface coating through polymerization of the adjacently grafted dopamine molecules. It should be noted that the microstructure of polydopamine can vary from monomer to monomer unit, where quinone, indole, and quinhydrone-derived moieties may exist, although their favorable intermolecular interactions contribute to not only the robustness of the bio-inspired resin,<sup>[14]</sup> but can even contribute to enhanced hemocompatibility.<sup>[15]</sup>

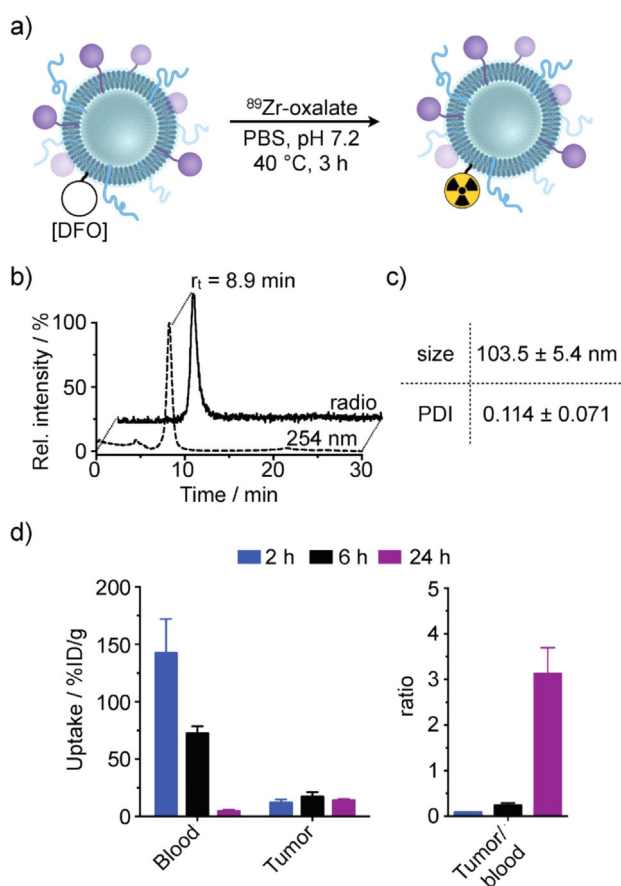


**Figure 2.** Synthesis, chemical characterization, and in vivo biodistribution of  $^{89}\text{Zr}$ -labeled TCO-functionalized liposomal nanoparticles. a) Formulation and radiolabeling. b) UV (254 nm) and radio-chromatogram by size exclusion chromatography. c) Analysis of size and polydispersity of  $^{89}\text{Zr}$ -labeled liposomal nanoparticle. d) In vivo biodistribution of  $^{89}\text{Zr}$ -TCO liposomal nanoparticles in 4T1-tumor-bearing nude mice.

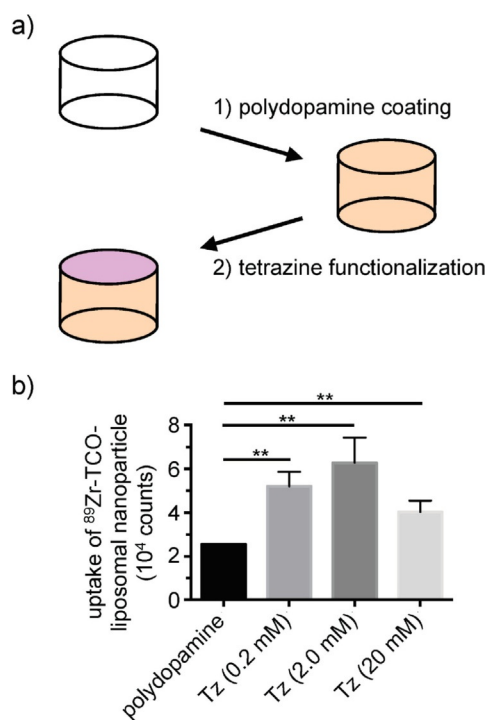


**Figure 3.** Synthesis and optimization of a tetrazine-functionalized polydopamine-coated CoCrMo stent alloy (Tz-PDA@CoCrMo). a) A schematic illustration of thin-film deposition of polydopamine and tetrazine functionalization through amide-bond formation. b) Retention of <sup>89</sup>Zr-TCO liposomal nanoparticles at different concentrations of Tz NHS ester on tetrazine functionalized of polydopamine-coated metal disks.

The grafted amines were converted in the second step to tetrazine-appended amides by using *N*-hydroxysuccinimide-displacement chemistry. The amide-bound tetrazines can selectively “click” with *trans*-cyclooctene groups on substrates such as liposomes (Figure 3B), immobilizing the macromolecular carriers and potentially removing them from circulation. Different concentrations of Tz-NHS ester solutions (0.2 mM, 2.0 mM, and 20 mM) were evaluated for the functionalization of PDA@CoCrMo-alloy disks to achieve maximum deposition of Tz functionalities on the polydopamine-coated metal surface. After tetrazine functionalization, Tz-PDA@CoCrMo disks ( $n=3$ ) were incubated with <sup>89</sup>Zr-TCO-liposomes at room temperature for 5 min and the bound activity was measured through  $\gamma$ -counting. In all cases, we observed a statistically significant increase in uptake of <sup>89</sup>Zr-TCO-liposomal nanoparticles on the Tz-functionalized CoCrMo alloy disks (Tz-PDA@CoCrMo) in comparison to PDA@CrCoMo metal disks, demonstrating the successful deposition of tetrazine functionalities on the polydopamine-coated metal disks. However, no statistical difference between the different concentrations of Tz-NHS ester was observed.

The viability of a conceptual liposome “filter” that could be suitable as a stent material was evaluated through radiolabeling efficiencies of CoCrMo alloy disks of various coatings (Figure 4). The tetrazine-appended polydopamine-coated CoCrMo surface (Tz-PDA@CoCrMo) was treated with a buffered radiolabeled TCO-functionalized liposome formulation as well as non-TCO functionalized <sup>89</sup>Zr-labeled liposomes (Figure 4A),

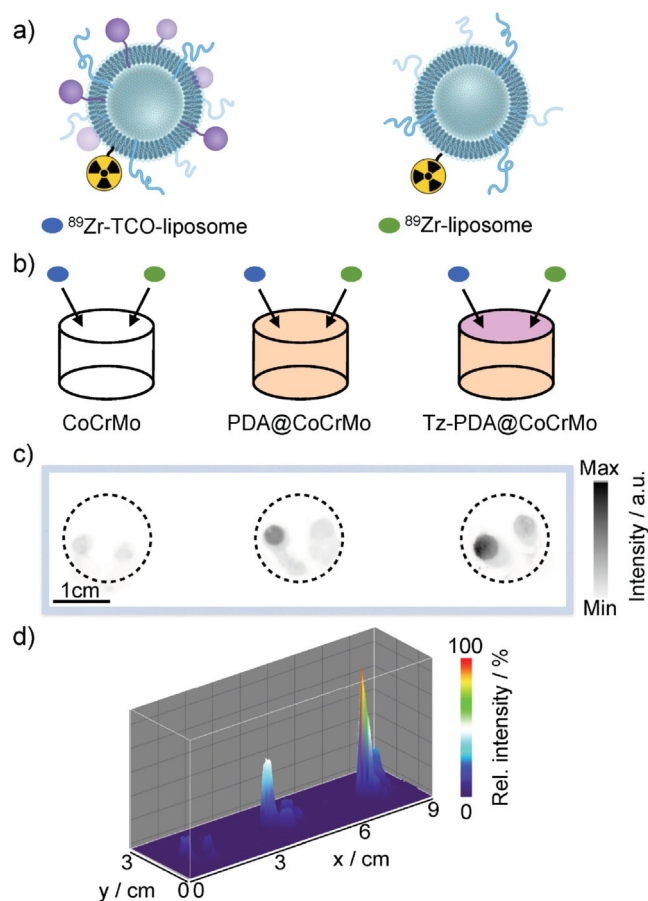


**Figure 4.** Comparison in uptake of <sup>89</sup>Zr-TCO-liposomal nanoparticles versus <sup>89</sup>Zr-liposomal nanoparticles on CoCrMo alloy stent surfaces. a) Synthesis of TCO-functionalized and non-TCO-functionalized <sup>89</sup>Zr-labeled liposomal nanoparticles. b) Schematic illustration of the experimental setup. c, d) Analysis of bound activity of <sup>89</sup>Zr-labeled nanoparticles by phosphor autoradiography.

and was left to stand for 5 min prior to a rinse to remove residual “unbound” liposomes (Figure 4B). The amount of radioactivity retained was compared to a bare CoCrMo alloy and a non-tetrazine-functionalized PDA@CoCrMo, both of which were treated with the same radiolabeled liposome solutions. Figure 4C depicts phosphor autoradiography films displaying the radioactivity that had remained on the disk surfaces. Four times less radioactivity was retained on the bare CoCrMo alloy compared to the Tz-functionalized disks with the highest activity, suggesting that the TCO-tetrazine click reaction is responsible for the enhanced uptake of the liposomes. Although considerably more radioactivity was retained on the tetrazine-functionalized PDA@CoCrMo disk, a two-fold decrease in the amount was still observed on the disk that was not treated with Tz NHS-ester. This could be because of side reactions of the strained *Z*-isomer of the cyclooctene, which can include Michael addition to the polydopamine amine or even Diels–Alder couplings with catechol-derived quinone dienes.<sup>[14]</sup> Owing to the bioorthogonal click reaction, the majority of PDA–liposome binding originates from the positively charged polydopamine surface itself, which may have an inherent electrostatic affinity for the negatively charged liposomes.

In summary,  $^{89}\text{Zr}$ -radiolabeled TCO-functionalized liposomal nanoparticles ( $^{89}\text{Zr}$ -TCO-LNP) with good in vivo pharmacokinetics were prepared for selective binding to a rationally engineered tetrazine-appended polydopamine-coated CoCrMo alloy disk. We have shown specific binding between these two counterparts through the rapid bioorthogonal inverse electron-demand Diels–Alder click reaction between tetrazines and *trans*-cyclooctenes. This report represents the first steps taken towards a new technology of on-demand removal of circulating liposomal nanoparticles in vivo.

## Experimental Section

### Materials

Unless otherwise stated, all chemicals and solvents were used without further purification. Water used for this study was ultrapure ( $> 18.2 \text{ M}\Omega \text{ cm}^{-1}$  at  $25^\circ\text{C}$ ), and acetonitrile ( $\text{CH}_3\text{CN}$ ) as well as ethanol were of HPLC grade purity. L-Dopamine hydrochloride, Trizma<sup>®</sup> base, *p*-benzylamino tetrazine *N*-hydroxysuccinimidyl ester (Tz NHS ester), triethylamine, and dimethylformamide were purchased from Sigma–Aldrich (USA) and used as received. Phospholipids were purchased from Avanti polar Lipids. Cobalt chromium molybdenum alloy disks (CoCrMo, 63:30:7 wt%) were purchased from American Elements (CA, USA). TCO-NHS ester was purchased from KeraFast (MA, USA). Chelexed water was prepared with BT Chelex 100 Resin (Bio-Rad) and phosphate-buffered saline (PBS) was purchased from the media preparation facility at Memorial Sloan Kettering Cancer Center.  $^{89}\text{Zr}$ -oxalate was purchased from the radiochemistry core at Memorial Sloan Kettering Cancer Center. HPLC reactions and quality controls ( $1.0 \text{ mL min}^{-1}$ , phosphate-buffered saline) were performed on a Shimadzu UFLC HPLC system equipped with a DGU-20A degasser, a SPD-M20A UV detector, a LC-20AB pump system, a CBM-20A communication BUS module, and a Scan-RAM radio-TLC/HPLC-detector from Lablogic using a size exclusion column (GE Superdex<sup>™</sup> 200, 10/300 GL). Electrospray ionization mass spectrometry (ESI-MS) spectra were recorded with a Waters Acquity UPLC (Milford, CA) with electrospray ionization SQ detector. Size and zeta potential measurements were performed on a Malvern Zetasizer NanoSeries.

### Formulation of TCO-Functionalized Liposomal Nanoparticles

The formulation of TCO-functionalized liposomal nanoparticles is based on a previously established protocol.<sup>[4]</sup> In detail, the liposomal nanoparticle suspension consisting of 1,2-dipalmitoyl-*sn*-glycero-3-phosphocholine (DPPC), cholesterol, pegylated DSPE (DSPE-PEG2000), DSPE-TCO, and DSPE-DFO in a 1.85:1:0.15:0.03:0.01 molar ratio was prepared by adding the individual lipids to a reaction vessel in a solution of chloroform. After removing the organic solvent under reduced pressure, the resulting lipid film was dried under high vacuum for 2 h. Phosphate-buffered saline (pH 7.4, 4.0 mL) was added to the reaction vessel and stirred at  $40^\circ\text{C}$  for 1 h. Followed by tip sonication and centrifugation, TCO-functionalized liposomal nanoparticles were isolated and stored as a suspension in PBS. Particle diameters were measured to be  $109.4 \pm 8.8 \text{ nm}$  ( $n=3$ ) with a polydispersity index [PDI] of  $0.153 \pm 0.027$  ( $n=3$ ) and a zeta potential of  $-6.8 \pm 4.4 \text{ mV}$  ( $n=3$ ). Non-functionalized liposomal nanoparticle suspensions without the DSPE-TCO constituent were prepared as control formulations and exhibited analogous properties to those reported by Perez et al.<sup>[4]</sup>

### Radiolabeling of $^{89}\text{Zr}$ -TCO-Liposomes

$^{89}\text{Zr}$ -oxalate ( $7.3 \mu\text{L}$ ,  $98 \mu\text{Ci}$ ) was added to phosphate-buffered saline ( $100 \mu\text{L}$ ) and the pH was adjusted to 7.5 by adding  $\text{Na}_2\text{CO}_3$  ( $1 \text{ M}$ ,  $7.0 \mu\text{L}$ ). After the addition of a solution of TCO-liposomal nanoparticles ( $100 \mu\text{L}$ ), the reaction mixture was incubated at  $40^\circ\text{C}$  for 1 h. After purification by sequential spin filtration ( $5\times$ ) using Amicon<sup>®</sup> filters ( $100 \text{ kDa}$ , EMD Millipore),  $^{89}\text{Zr}$ -TCO-liposomal nanoparticles were isolated ( $49 \pm 5\%$  radiochemical yield,  $> 97\%$  radiochemical purity,  $n=5$ ) with similar characteristics (size:  $103.5 \pm 5.4 \text{ nm}$  and PDI:  $0.114 \pm 0.071$ ,  $n=3$ ) as their precursors.

### Biodistribution of $^{89}\text{Zr}$ -TCO-Liposomes

Evaluating the in vivo performance of  $^{89}\text{Zr}$ -TCO-liposomes, 4T1-tumor-bearing ( $150\text{--}200 \text{ mm}^3$ ) mice (female, nude, 6–8 weeks, 20–25 g) were intravenously injected with a solution of  $^{89}\text{Zr}$ -TCO-liposomes ( $13.3\text{--}18.2 \mu\text{Ci}$ ,  $0.5 \mu\text{mol}$  of lipid) in PBS ( $150 \mu\text{L}$ ). At predetermined time points (2, 6, and 24 h post-injection), the mice were euthanized by asphyxiation with  $\text{CO}_2$  and blood was collected via cardiac puncture. Selected organs were harvested, weighed, and counted by using a Wizard<sub>2</sub> automatic  $\gamma$ -counter from PerkinElmer. The percentage of tracer uptake stated as percentage injected dose per gram of tissue ( $\% \text{IDg}^{-1}$ ) was calculated as the activity bound to tissue per organ weight per actual injected dose, decay-corrected to the start time of counting. All animal experiments were approved by the Institutional Animal Care and Use Committee (IACUC) of Memorial Sloan Kettering Cancer Center.

### Preparation of Tetrazine-Functionalized Stent Alloy

Functionalization of commercial CoCrMo alloy disks was achieved by coating the surface with a polydopamine coating using a modified literature protocol.<sup>[12]</sup> Amidization of surface amines through *N*-hydroxysuccinimide (NHS) displacement yields tetrazine covalencies. The alloy disk was first surface-treated with piranha solution (3:1 w/w  $\text{H}_2\text{SO}_4$  [conc.]/ $\text{H}_2\text{O}_2$  [30% w/w]) for 16 h. After rinsing with water, the disk was submerged in a freshly prepared aqueous solution of Trizma<sup>®</sup> base ( $1.2 \text{ mg mL}^{-1}$ ) and dopamine ( $2 \text{ mg mL}^{-1}$ ) (pH 8.5) and agitated at  $20^\circ\text{C}$  for 16 h. After rinsing with water, the disks were cured at  $150^\circ\text{C}$  for 1 h. The resulting polydopamine-coated disks (PDA@CoCrMo) were then incubated in the dark at  $20^\circ\text{C}$  with layer of pipette-dropped solutions of Tz NHS ester (0.2 mm, 2.0 mm, or 20 mm) and triethylamine (0.15 mm) for 1 h prior to a water rinse to afford the tetrazine-appended surface-coated alloy (Tz-PDA@CoCrMo). Then, the reaction solution was removed by washing with water ( $3 \times 1.0 \text{ mL}$ ).

### Optimization of Tetrazine Functionalization of Polydopamine-Coated CoCrMo Alloy Disks

After the dilution of  $^{89}\text{Zr}$ -TCO-liposomal nanoparticles ( $100 \mu\text{L}$ ,  $62 \mu\text{Ci}$ ) with PBS ( $1.0 \text{ mL}$ ), Tz-PDA@CoCrMo disks prepared under various Tz NHS ester conditions (0.2 mm, 2.0 mm, and 20 mm;  $n=3$ ) and non-functionalized PDA@CoCrMo disks ( $n=3$ ) were incubated with a solution of  $^{89}\text{Zr}$ -TCO-liposomal nanoparticles ( $100 \mu\text{L}$ ) for 5 min at  $20^\circ\text{C}$ . The disks were then carefully washed with PBS ( $10 \text{ mL}$ ) and residual radioactivity on the disks was measured by using a Wizard<sup>2</sup> automatic  $\gamma$ -counter from PerkinElmer.

## Comparison in Uptake of $^{89}\text{Zr}$ -TCO-Liposomal Nanoparticles and $^{89}\text{Zr}$ -Liposomal Nanoparticles

For digital autoradiography experiments, bare CoCrMo, PDA@CoCrMo, and Tz-PDA@CoCrMo disks were incubated with pipette-delivered drops of  $^{89}\text{Zr}$ -TCO-liposomal nanoparticles (2  $\mu\text{L}$ , 2.0  $\mu\text{Ci}$ ) or  $^{89}\text{Zr}$ -liposomal nanoparticles (2  $\mu\text{L}$ , 2.0  $\mu\text{Ci}$ ) for 5 min at 20 °C (Figure 4A and Figure 4B). After washing with PBS (10 mL), bound radioactivity on the metal disks was measured by exposing them to a phosphor-imaging plate (Fujifilm, BAS-MS2325, Fuji Photo, Japan) for 24 h at 20 °C. After exposure, the imaging plate was analyzed by using a Typhoon FLA 7000 laser scanner (GE Healthcare, Port Washington, NY) with 25  $\mu\text{m}$  pixel resolution.

## Acknowledgements

This work was supported by a Center for Molecular Imaging & Nanotechnology grant of Memorial Sloan Kettering Cancer Center (to T.R.); NIH R01 EB017748 and K08 CA16396 (to M.F.K.); M.F.K. is a Damon Runyon-Rachleff Innovator supported (in part) by the Damon Runyon Cancer Research Foundation (DRR-29-14). The authors thank the Small Animal Imaging Core and the Radiochemistry and Molecular Imaging Probes Core for support (P30 CA008748).

## Conflict of Interest

The authors declare no conflict of interest.

**Keywords:**  $^{89}\text{Zr}$  · click chemistry · CoCrMo alloys · liposomes · tetrazine · trans-cyclooctene

- [1] A. L. Petersen, A. E. Hansen, A. Gabizon, T. L. Andresen, *Adv. Drug Delivery Rev.* **2012**, *64*, 1417–1435.

- [2] J. Marik, M. S. Tartis, H. Zhang, J. Y. Fung, A. Kheiruloomoo, J. L. Sutcliffe, K. W. Ferrara, *Nucl. Med. Biol.* **2007**, *34*, 165–171.
- [3] C. Pérez-Medina, D. Abdel-Atti, J. Tang, Y. Zhao, Z. A. Fayad, J. S. Lewis, W. J. M. Mulder, T. Reiner, *Nat. Commun.* **2016**, *7*, 11838–11846.
- [4] C. Pérez-Medina, D. Abdel-Atti, Y. Zhang, V. A. Longo, C. P. Irwin, T. Binderup, J. Ruiz-Cabello, Z. A. Fayad, J. S. Lewis, W. J. M. Mulder, T. Reiner, *J. Nucl. Med.* **2014**, *55*, 1706–1711.
- [5] S. G. Lee, K. Gangangari, T. M. Kalidindi, B. Punzalan, S. M. Larson, N. V. Pillarsetty, *Nucl. Med. Biol.* **2016**, *43*, 781–787.
- [6] Y. Matsumura, H. Maeda, *Cancer Res.* **1986**, *46*, 6387–6392.
- [7] T. van der Geest, P. Laverman, J. M. Metselaar, G. Storm, O. C. Boerman, *Expert Opin. Drug Delivery* **2016**, *13*, 1231–1242.
- [8] M. Patra, K. Zarschler, H.-J. Pietzsch, H. Stephan, G. Gasser, *Chem. Soc. Rev.* **2016**, *45*, 6415–6431.
- [9] a) N. K. Devaraj, R. Weissleder, *Acc. Chem. Res.* **2011**, *44*, 816–827; b) M. R. Karver, R. Weissleder, S. A. Hilderbrand, *Bioconjugate Chem.* **2011**, *22*, 2263–2270; c) A. C. Knall, C. Slugovc, *Chem. Soc. Rev.* **2013**, *42*, 5131–5142.
- [10] a) B. M. Zeglis, K. K. Sevak, T. Reiner, P. Mohindra, S. Carlin, P. Zanzonico, R. Weissleder, J. S. Lewis, *J. Nucl. Med.* **2013**, *54*, 1389–1396; b) B. M. Zeglis, P. Mohindra, G. I. Weissmann, V. Divilov, S. A. Hilderbrand, R. Weissleder, J. S. Lewis, *Bioconjugate Chem.* **2011**, *22*, 2048–2059; c) P. Adumeau, K. E. Carnazza, C. Brand, S. D. Carlin, T. Reiner, B. J. Agnew, J. S. Lewis, B. M. Zeglis, *Theranostics* **2016**, *6*, 2267–2277.
- [11] a) J. L. Houghton, R. Membreno, D. Abdel-Atti, K. M. Cunanan, S. D. Carlin, W. W. Scholz, P. B. Zanzonico, J. S. Lewis, B. M. Zeglis, *Mol. Cancer Ther.* **2017**, *16*, 124–133; b) R. Rossin, T. Lappchen, S. M. van den Bosch, R. Laforest, M. S. Robillard, *J. Nucl. Med.* **2013**, *54*, 1989–1995.
- [12] J. Sobocinski, W. Laure, M. Taha, E. Courcot, F. Chai, N. Simon, A. Addad, B. Martel, S. Haulon, P. Woisel, N. Blanchemain, J. Lyskawa, *ACS Appl. Mater. Interfaces* **2014**, *6*, 3575–3586.
- [13] a) Q. Ye, F. Zhou, W. Liu, *Chem. Soc. Rev.* **2011**, *40*, 4244–4258; b) H. Lee, S. M. Dellatore, W. M. Miller, P. B. Messersmith, *Science* **2007**, *318*, 426–430.
- [14] S. R. Nielsen, F. Besenbacher, M. Chen, *Phys. Chem. Chem. Phys.* **2013**, *15*, 17029–17037.
- [15] R. Luo, L. Tang, S. Zhong, Z. Yang, J. Wang, Y. Weng, Q. Tu, C. Jiang, N. Huang, *ACS Appl. Mater. Interfaces* **2013**, *5*, 1704–1714.

Received: May 26, 2017

Version of record online August 7, 2017